New Phytologist

Research

Environmentally driven evolution of Rubisco and improved photosynthesis and growth within the C_3 genus *Limonium* (Plumbaginaceae)

Jeroni Galmés[1], P. John Andralojc[2], Maxim V. Kapralov[3], Jaume Flexas[1], Alfred J. Keys[2], Arántzazu Molins[1], Martin A. J. Parry[2] and Miquel À. Conesa[1]

[1]Research Group on Plant Biology under Mediterranean Conditions, Universitat de les Illes Balears, Balearic Islands, Spain; [2]Plant Biology & Crop Science, Rothamsted Research, Harpenden AL5 2JQ, UK; [3]Plant Science Division, Research School of Biology, The Australian National University, Canberra, ACT 0200, Australia

Author for correspondence:
Jeroni Galmés
Tel: +34 971259720
Email: jeroni.galmes@uib.cat

Received: *16 February 2014*
Accepted: *23 April 2014*

New Phytologist (2014) **203:** 989–999
doi: 10.1111/nph.12858

Key words: carboxylase catalytic efficiency, drought, evolution, improved photosynthesis, *Limonium*, Mediterranean, Rubisco, water stress.

Summary

- Carbon assimilation by most ecosystems requires ribulose-1,5-bisphosphate carboxylase/oxygenase (Rubisco). Its kinetic parameters are likely to have evolved in parallel with intracellular CO_2 availability, with the result that faster forms of Rubisco occur in species with CO_2-concentrating mechanisms.
- The Rubisco catalytic properties were determined and evaluated in relation to growth and carbon assimilation capacity in Mediterranean *Limonium* species, inhabiting severe stress environments.
- Significant kinetic differences between closely related species depended on two amino acid substitutions at functionally important residues 309 and 328 within the Rubisco large subunit. The Rubisco of species facing the largest CO_2 restrictions during drought had relatively high affinity for CO_2 (low Michaelis–Menten constant for CO_2 (K_c)) but low maximum rates of carboxylation (k^c_{cat}), while the opposite was found for species that maintained higher CO_2 concentrations under similar conditions. Rubisco kinetic characteristics were correlated with photosynthetic rate in both well-watered and drought-stressed plants. Moreover, the drought-mediated decrease in plant biomass accumulation was consistently lower in species with higher Rubisco carboxylase catalytic efficiency (k^c_{cat} /K_c).
- The present study is the first demonstration of Rubisco adaptation during species diversification within closely related C_3 plants, revealing a direct relationship between Rubisco molecular evolution and the biomass accumulation of closely related species subjected to unfavourable conditions.

Introduction

The photosynthetic processes that are most vulnerable to high temperature and drought remain unclear and somewhat controversial (Salvucci & Crafts-Brandner, 2004; Schrader *et al.*, 2004; Yamori *et al.*, 2010). However, factors related to the performance of a key photosynthetic enzyme, ribulose-1,5-bisphosphate carboxylase/oxygenase (Rubisco), undoubtedly contribute to the restricted yields associated with elevated temperature and water deficit (Sharkey, 2005; Sage & Kubien, 2007). Rubisco provides a ubiquitous gateway for the entry of inorganic carbon (as CO_2) into plant metabolism, yet cannot fully discriminate between CO_2 and O_2 as it catalyses the chemical combination of either gaseous substrate with an enediolate form of the Calvin cycle intermediate ribulose-1,5-bisphosphate (RuBP). The oxygenation of RuBP gives rise to the energy-dissipating process of photorespiration, and increases steeply in extent with increasing temperature and water stress, reducing plant productivity. Significant progress has been made in understanding the components that determine the fundamental properties of Rubisco at a molecular level (Spreitzer & Salvucci, 2002; Parry *et al.*, 2013), such as the driving forces behind the evolutionary adaptation of Rubisco (Raven, 2000; Tcherkez *et al.*, 2006), the trade-offs involved in determining the magnitude of its kinetic parameters (Savir *et al.*, 2010; Tcherkez, 2013; Galmés *et al.*, 2014), and the underlying structural dynamics (Bracher *et al.*, 2011; van Lun *et al.*, 2011, 2014). Strong evidence for widespread amino acid sequence coevolution and for the role of positive selection in the evolutionary fine-tuning of Rubisco from both C_3 and C_4 plants has been reported in recent phylogenetic studies (Kapralov & Filatov, 2007; Christin *et al.*, 2008; Kapralov *et al.*, 2011, 2012; Wang *et al.*, 2011; Young *et al.*, 2012). Genetic transformation of *Chlamydomonas* has helped to elucidate the roles of particular Rubisco domains (Meyer *et al.*, 2012; Esquivel *et al.*, 2013), while new molecular tools have facilitated the modification of Rubisco *in planta*, enabling the effect of specific amino acid

substitutions on Rubisco kinetics to be evaluated (Whitney *et al.*, 2011). However, there are still insufficient data to establish the way in which the kinetic properties of Rubisco impact upon the capacity for CO_2 assimilation and the overall plant carbon balance under challenging environmental conditions.

Extreme environments are particularly useful in the study of adaptive evolution in plants. Intense selection pressure not only increases the frequency of adaptation but can also lead to the emergence of alternative survival strategies (Agrawal *et al.*, 2009; Adler *et al.*, 2014). Species of the genus *Limonium* Mill. (Plumbaginaceae, Caryophyllales) inhabit Mediterranean coastal habitats, which are characterized by low soil osmotic potential as a result of negative water balance and the continuous influx of salt from marine spray. Low atmospheric and soil water potentials require strict control of water loss through transpiration, by means of stomatal closure. Diminished stomatal conductance (g_s) is often accompanied by decreased leaf mesophyll conductance to CO_2 (g_m), which in turn limits the availability of CO_2 to Rubisco in the chloroplast stroma, favouring RuBP oxygenation (Flexas *et al.*, 2013). The high ambient temperatures and elevated solar irradiance typical of these xeric environments further increase photorespiration, which may compromise plant carbon balance and, ultimately, survival.

Here we integrate data on Rubisco kinetics, leaf photosynthesis and plant growth under irrigated and severe drought conditions for a number of species of the genus *Limonium*. *Limonium* species from the Balearic Islands are an ideal model system in which to study the link between drought tolerance and Rubisco kinetics for several reasons. First, the genus *Limonium*, with up to 300 species, represents one of the largest radiations in the Mediterranean Basin (Erben, 1993). The Balearic Islands are home to 42 *Limonium* species, most of them being endemics with a narrow distribution (Erben, 1993; Rosselló & Sáez, 2001) that have evolved as a recent radiation (reviewed in Lledó *et al.*, 2005). Secondly, drought-tolerant *Limonium* species have adapted to the hostile environments of coastal margins (Galmés *et al.*, 2011a), where biotic competition is virtually absent as a result of extreme abiotic stress factors such as lack of fresh water, high temperature and excess solar radiation. Finally, there is significant diversity in Rubisco kinetics among *Limonium*, with *Limonium gibertii* (Sennen) Sennen having among the highest specificities for CO_2 reported in terrestrial plants (Galmés *et al.*, 2005). Furthermore, biochemical modelling predicts that significant yield increases would ensue if *L. gibertii* Rubisco were to replace the native wheat counterpart (Parry *et al.*, 2011).

In the present work, we sampled all *Limonium* species inhabiting the Balearic Islands and assessed the amino acid sequence polymorphisms in the Rubisco large subunit (L-subunit). Full kinetic characterization of Rubisco was performed for 14 of these species, representing all of the amino acid polymorphisms found. Further, photosynthetic performance and plant growth were assessed for these species under well-watered (WW) and severe water stress (WS) conditions. Our results demonstrate a correlation between drought tolerance, photosynthetic performance and Rubisco catalytic efficiency. We also identified two L-subunit amino acid substitutions that were probably responsible for changes in Rubisco kinetic properties, and assessed the ecological success of *Limonium* species with different L-subunits.

Materials and Methods

Species sampling

All cited and described *Limonium* species reliably recognized in the Balearic Islands (Erben, 1993; Rosselló & Sáez, 2001) were included in the survey, resulting in sampling plants from 47 populations which represented 42 *Limonium* species (Fig. 1). Several populations were sampled for species occurring in different islands, occurring in extremes of an island, or showing notorious differences in plant morphology. The locations of sampled populations are shown in Fig. 1. In addition to the 47 populations of *Limonium*, we also sampled *Myriolimon ferulaceum* (L.) Lledó, Erben & M.B. Crespo, the monotypic genus sister to *Limonium*, which served as an outgroup. Fresh leaf tissue and seeds from five plants per population were sampled in the field and dried in silica gel for further DNA sequencing and the drought experiment, respectively.

*rbc*L sequences and phylogenetic analyses

Total DNA was extracted from fresh leaves using the DNeasy Plant MiniKit (Qiagen). The *rbc*L gene coding for the Rubisco L-subunit was amplified and sequenced using the forward primer *rbc*L1F (5′-ATGTCACCACAAACAGAAACT-3′) and a newly designed reverse primer (5′-AGTATCCATTGCGGCGAATT-3′), following the protocol in Kapralov & Filatov (2006). All polymorphic sites were checked against the original sequence chromatograms and doubtful regions were re-sequenced; sequences were compared with homologues from GenBank, and open reading frame (ORF) integrity was confirmed. Novel sequences have been submitted to GenBank under accession numbers KJ608007–KJ608054. Sequences were aligned and phylogenetic reconstructions were performed using maximum likelihood (ML) and maximum parsimony (MP) algorithms, both with 1000 bootstrap resamplings, implemented in MEGA 5.1 (Tamura *et al.*, 2011), and Bayesian analyses (Markov chain Monte Carlo method), with 10^6 bootstrap generations, implemented in MRBAYES 3.1.2 (Huelsenbeck & Ronquist, 2001). The trees were rooted using *M. ferulaceum*. All methods produced trees with identical topology but minor differences in bootstrap values.

Identification of Rubisco residues under positive selection

We analysed variation in the ratio of nonsynonymous to synonymous substitution rates (d_N/d_S) across *rbc*L codons and/or particular branches of phylogenies using models *M8* and *A* from the *codeml* program of the PAML package v.4 (Yang, 1997, 2007). Posterior probabilities that a certain amino acid belongs to a class with $d_N/d_S > 1$ and hence is under positive selection were calculated using the Bayes Empirical Bayes approaches implemented in PAML (Yang *et al.*, 2005). Because all Balearic *Limonium rbc*L sequences were clustered into three groups without

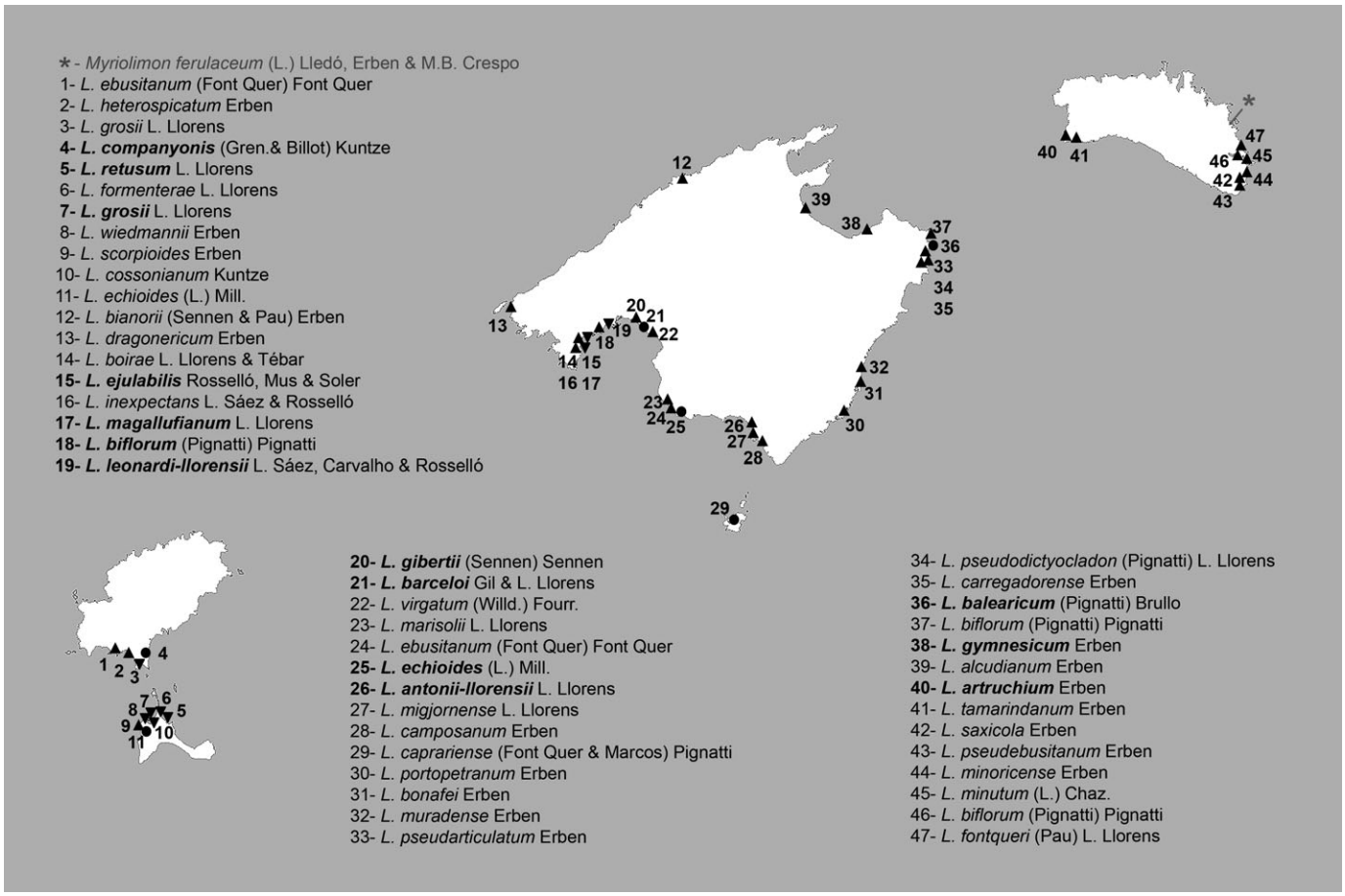

Fig. 1 Map of the Balearic Islands showing locations of the sampled populations for each species. Rubisco large subunit (L-subunit) haplotypes are indicated as circles for haplotype I, triangles, apex down for haplotype II, and triangles, apex up for haplotype III. Populations used in the drought experiment are indicated in bold. The outgroup *Myriolimon ferulaceum*, with an L-subunit haplotype not corresponding to I, II or III, is indicated in grey (*).

nonsynonymous variation within them, we only used one sequence per group plus the sequence of *M. ferulaceum.* One needs at least seven sequences or preferably more to overcome the problem of false negatives in *codeml* (Anisimova *et al.*, 2001). Therefore, in addition to four *rbc*L sequences representing Balearic Plumbaginaceae, we used seven *rbc*L sequences from GenBank which represented Plumbaginaceae species occurring in communities of drought-resistant plants in regions with a Mediterranean climate similar to that experienced by Balearic *Limonium* species (Kubitzki *et al.*, 1993): *Armeria bottendorfensis* A. Schulz (Z97640), *Armeria splendens* Boiss. (Y16908), *Limoniastrum monopetalum* Boiss. (Z97642), *Limonium sinuatum* (L.) Mill. (Y16900), *Limonium spectabile* (Svent.) G. Kunkel & Sunding (Z97646), *Plumbago auriculata* Lam. (EU002283) and *Plumbago capensis* Thunb. (Y16906). Using such a broad outgroup also allowed the establishment of ancestral states for polymorphic amino acid residues. PAML analyses were run on an unrooted phylogeny (Fig. 2a; spinach (*Spinacia oleracea* L.) was not included in the analyses) which was reconstructed using ML and only synonymous sites to avoid distortion caused by possible positive selection on *rbc*L (Kapralov & Filatov, 2007). Models *M8* and *A* assumed selection across all branches and selected foreground branches only, respectively. Branches leading to all Balearic *Limonium* haplotypes and to derived haplotypes II and III only were selected as foreground branches in two separate tests for positive selection allowing d_N/d_S ratios to vary both among sites and among lineages.

We also inferred ancestor Rubisco L-subunit protein sequences for each interior node of the analysed Plumbaginaceae *rbc*L tree using the PAML package v.4 (Yang, 1997, 2007) and looked for parallel or convergent amino acid changes, in which changes along independent lineages have occurred from the same or different ancestral amino acids, respectively (Zhang & Kumar, 1997).

Drought treatment and growth analysis

Based on the three different Rubisco L-subunit haplotypes detected within *Limonium*, the following 14 species were selected for the drought experiment: *Limonium balearicum*, *Limonium barceloi*, *Limonium companyonis* and *Limonium echioides* representing haplotype I; *Limonium ejulabilis*, *Limonium grosii*, *Limonium leonardi-llorensii*, *Limonium magallufianum* and *Limonium retusum* representing haplotype II; *Limonium antonii-llorensii*, *Limonium artruchium*, *Limonium biflorum*, *Limonium gibertii* and *Limonium gymnesicum* representing haplotype III. Populations used for each species and their

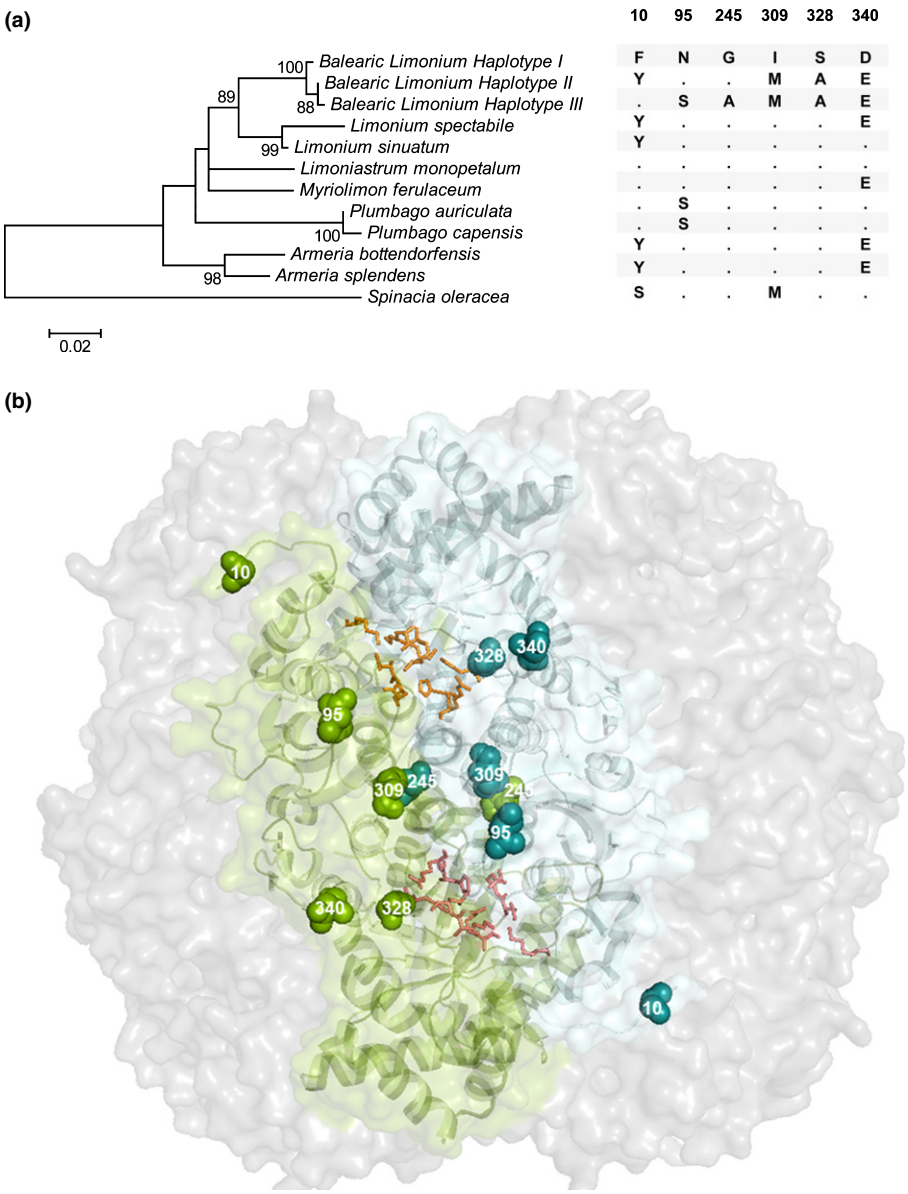

Fig. 2 *Limonium* Rubisco large subunit (L-subunit) sequence variation and structural location of polymorphic residues. (a) Maximum likelihood tree inferred from the *rbc*L gene coding for the L-subunit for Plumbaginaceae species used in the analyses of positive selection. *Spinacia oleracea* was added as an outgroup and for comparative purposes; it was not included in the positive selection analysis. Bootstrap values (from 1000 replicates) are indicated at the nodes. Amino acid polymorphism of six Rubisco L-subunit residues that varied in Balearic *Limonium* is shown on the right. Residue numbers are shown above the table. Residues identical to those of the first sequence are shown as dots. (b) Location of the six polymorphic Rubisco L-subunit residues shown on the structure of spinach Rubisco (1UPM). Two L-subunits forming a functional dimer are highlighted in green and cyan. Residues forming two active sites are shown in orange; six polymorphic residues are shown as green and cyan spheres for L-subunits B and L, respectively.

locations are indicated in Fig. 1 (including species authorities). In these populations, seeds were collected from several plants. Thereafter, 10 plants per species were grown from seeds outdoors in 3-l pots with water supplied at field capacity under typical Mediterranean summer conditions. Three months after germination, and to the end of the experiment, five plants per species were subjected to severe water stress by maintaining the pots at 10–30% of field capacity (WS), whereas the remaining plants were maintained at field capacity (WW). Pots were weighed every 2–3 d to enable replacement of lost water. Three months after drought treatment application, plants were harvested to obtain total plant biomass.

Leaf gas exchange and chlorophyll fluorescence measurements

Leaf gas exchange and chlorophyll fluorescence were measured in all species and treatments included in the drought experiment except for *L. artruchium* and *L. gymnesicum*, because of their small leaves. Measurements were performed 2 months after the onset of the drought treatment, that is, in leaves completely developed under treatment. The net CO_2 assimilation rate (A_N) was measured at mid-morning in fully expanded leaves using a gas-exchange analyser equipped with a leaf chamber fluorometer (Li-6400-40; Li-Cor Inc., Lincoln, NE, USA). Leaf chamber conditions consisted

of a photosynthetic photon flux density of 1500 μmol m^{-2} s^{-1} (with 10% blue light to induce stomatal aperture) and an ambient CO_2 concentration of 400 μmol mol^{-1}. Leaf temperature during measurements was maintained at 25°C.

The quantum efficiency of the photosystem II (PSII)-driven electron transport was determined using the equation:

$$\phi_{PSII} = (F'_m - F_s)/F'_m \quad \text{Eqn 1}$$

(F_s, the steady-state fluorescence in the light; F'_m, the maximum fluorescence obtained with a light-saturating pulse (10 000 μmol quanta m^{-2} s^{-1}) (Genty *et al.*, 1989)). As ϕ_{PSII} represents the number of electrons transferred per photon absorbed by PSII, the rate of electron transport (ETR) can be calculated as:

$$ETR = \phi_{PSII} \cdot PPFD \cdot \alpha \cdot \beta \quad \text{Eqn 2}$$

(α, the leaf absorbance; β, the distribution of absorbed energy between the two photosystems). The product $\alpha \cdot \beta$ was determined from the relationship between ϕ_{PSII} and ϕ_{CO_2} obtained by varying light intensity under nonphotorespiratory conditions in a nitrogen atmosphere containing < 1% (v/v) O_2 (Valentini *et al.*, 1995). ϕ_{CO_2} was calculated from gas-exchange measurements as $(A_N + R_L)$/PPFD, assuming that the rate of nonphotorespiratory CO_2 evolution in the light (R_L) was half of the dark mitochondrial respiration rate, R_{dark} (Galmés *et al.*, 2011b). R_{dark} was measured at pre-dawn at an ambient CO_2 concentration (C_a) of 400 μmol mol^{-1} and an air temperature of 25°C. The gross CO_2 assimilation rate (A_G) was obtained as $A_N + R_L$.

From combined gas-exchange and chlorophyll *a* fluorescence measurements, mesophyll conductance for CO_2 (g_m) was estimated according to Harley *et al.* (1992) as:

$$g_m = A_N/(C_i - (\Gamma * (ETR + 8\ (A_N + R_L)))/(ETR - 4\ (A_N + R_L))) \quad \text{Eqn 3}$$

The chloroplast CO_2 compensation point (Γ*) was calculated from the *in vitro* Rubisco specificity factor ($S_{c/o}$) values for each species as:

$$\Gamma* = 0.5O/S_{c/o} \quad \text{Eqn 4}$$

(O, the partial pressure of oxygen concentration in air (200 mbar)). Finally, from g_m estimates, the substomatal CO_2 concentration (C_i) values were transformed into chloroplastic CO_2 concentration (C_c) as:

$$C_c = C_i - (A_N/g_m) \quad \text{Eqn 5}$$

Rubisco catalytic characterization

Rubisco kinetic parameters were measured in the 14 species used in the growth experiment. Rates of Rubisco $^{14}CO_2$ fixation using fresh leaf protein extract were measured in 7-ml septum-capped scintillation vials, containing reaction buffer (yielding final concentrations of 100 mM Bicine-NaOH, pH 8.0, 20 mM $MgCl_2$, 0.4 mM RuBP and *c.* 100 W-A units of carbonic anhydrase) and one of nine different concentrations of CO_2 (0–80 μM, each with a specific radioactivity of 3.7×10^{10} Bq mol^{-1}), each at two concentrations of O_2 (0 and 21% (v/v)), as described previously (Parry *et al.*, 2007). Assays (1.0 ml total volume) were started by the addition of activated leaf extract, and the maximum velocity for carboxylase activity (V_{max}) together with the Michaelis–Menten constant (K_m) for CO_2 (K_c) determined from the fitted data. The K_m for the oxygenase activity was calculated from the relationship $K_{c,(21\%O_2)} = K_{c,(0\%O_2)} \cdot (1 + [O_2]/K_o)$. The $[O_2]$ was assumed to be 265 μM, but corrected for partial pressure by taking account of the atmospheric pressure and water saturated vapour pressure. Replicate measurements ($n = 3$–5) were made using protein preparations from two to 10 different leaves of different individuals. For each sample, the maximum rate of carboxylation (k^c_{cat}) was extrapolated from the corresponding V_{max} value after allowance was made for the Rubisco active site concentration, as determined by [^{14}C]CPBP binding (Yokota & Canvin, 1985). Rubisco CO_2/O_2 specificity ($S_{c/o}$) was measured as described previously (Galmés *et al.*, 2005) using enzyme purified by polyethylene glycol (PEG) precipitation and ion exchange chromatography, and the values given for each species were the mean of five to 10 repeated determinations. The maximum oxygenation rate (k^o_{cat}) was calculated using the equation $S_{c/o} = (k^c_{cat}/K_c)/(k^o_{cat}/K_o)$. All kinetic measurements were performed at 25°C.

Results

The molecular evolution of Rubisco in Balearic *Limonium* species

The 42 *Limonium* species (47 populations; Fig. 1) from the Balearic Islands possessed three Rubisco L-subunit amino acid haplotypes (haplotypes I, II and III) occurring in similar island habitats. Haplotype III, found in 29 species, was by far the most frequent in geographical distribution, while haplotypes I and II were found only in five and eight species, respectively (Fig. 1 and Supporting Information Fig. S1). The differences among haplotypes corresponded to polymorphisms at six L-subunit amino acid residues (Fig. 2a). Haplotypes I and II differed in four positions: F10Y, I309M, S328A and D340E; while haplotypes I and III differed in five positions: N95S, G245A, I309M, S328A and D340E (Fig. 2a). Phylogenetically, haplotype I appeared more basal than haplotypes II and III, when eight Plumbaginaceae species were included as the outgroup (Figs 2a, S1).

The implementing of Bayes Empirical Bayes analysis (Yang *et al.*, 2005) revealed that residues 309 and 328 were under positive selection along the branch leading to the Balearic *Limonium* haplotypes II and III, with posterior probabilities exceeding 0.95 (Fig. 2a). Amino acid substitutions I309M and S328A were unique to haplotypes II and III. No residues were shown to be under positive selection along the branch leading to all Balearic *Limonium* haplotypes (Fig. 2a). Site-specific tests revealed that residue 340 was under positive selection across all

investigated Plumbaginaceae, with a posterior probability of 0.93 (Fig. 2a).

Reconstruction of ancestral sequences for interior nodes was reliable; mean posterior probabilities for the entire protein exceeded 99% for all nodes. It confirmed that amino acid substitutions I309M and S328A occurred only once within analysed phylogeny (Fig. 2a) along the branch leading to the Balearic *Limonium* haplotypes II and III. Amino acid substitution G245A also occurred only once along the branch leading to the Balearic *Limonium* haplotype III. However, three other amino acid substitutions within the Balearic *Limonium* were not unique to this group. Parallel substitution F10Y occurred three times: along the branch leading to *Armeria* species, along the branch leading to *L. spectabile* and *L. sinuatum*, and also along the branch leading to the Balearic *Limonium* haplotype II. Parallel substitution N95S occurred twice along the branch leading to *Plumbago* species and the branch leading to the Balearic *Limonium* haplotype III. Parallel substitution E340D occurred four times: along the branch leading to the Balearic *Limonium* haplotype I, along the branch leading to *L. sinuatum*, along the branch leading to *L. monopetalum* and along the branch leading to the *Plumbago* species.

Species with different L-subunit haplotypes have different Rubisco kinetics

In order to investigate the impact of L-subunit substitutions on the catalytic properties of Rubisco, full kinetic characterization was undertaken for four to five species per haplotype (Table 1). Significant differences were observed between species. The Michaelis–Menten constant (K_m) for CO_2 (K_c) varied between 7.0 μM for *L. magallufianum* and 10.7 μM for *L. echioides* (Table 1). The species with the lowest Michaelis–Menten constant for O_2 (K_o) was *L. magallufianum* (297 μM), while the highest values were measured in *L. leonardi-llorensii* (438 μM). The maximum rate of carboxylation (k^c_{cat}) varied 2-fold, with the lowest values measured in *L. ejulabilis* (2.0 s^{-1}) and the highest in *L. echioides* (3.9 s^{-1}). Less variation was found in the carboxylation catalytic efficiency (k^c_{cat}/K_c), indicative of the inverse correlation between the rate of carboxylation and the affinity for CO_2. The Rubisco specificity factor ($S_{c/o}$) ranged between 103.3 mol mol^{-1} in *L. balearicum* and 121.2 mol mol^{-1} in *L. gymnesicum* (Table 1).

Significant kinetic differences were also found between the three haplotypes (Table 1), suggesting that the observed amino acid substitutions had catalytic consequences. Haplotype I Rubisco was faster (higher k^c_{cat}), but less specific for CO_2 (higher K_c and lower $S_{c/o}$) compared with haplotypes II and III (Table 1). Based on its higher value for k^c_{cat}/K_c, haplotype I represented superior carboxylation efficiency.

Highly significant relationships were found between the maximum rates of carboxylation (k^c_{cat}) and oxygenation (k^o_{cat}) (Table 1; $r^2 = 0.67$; $P < 0.001$), as well as between the carboxylase (k^c_{cat}/K_c) and the oxygenase (k^o_{cat}/K_o) catalytic efficiencies ($r^2 = 0.98$; $P < 0.001$). The greater k_{cat} and K_m values of haplotype I than of haplotypes II and III were paralleled by greater catalytic efficiencies (k_{cat}/K_m) for both the carboxylase and oxygenase reactions (Table 1). However, the relative change in catalytic efficiency for

Table 1 Comparison of Rubisco kinetics at 25°C for 14 species of *Limonium*, representing the three haplotypes identified

		Rubisco kinetic constants						
Haplotype	Species	K_c (μM)	K_o (μM)	k^c_{cat} (s^{-1})	k^c_{cat}/K_c (s^{-1} μM^{-1})	$S_{c/o}$ (mol mol^{-1})	k^o_{cat} (s^{-1})	k^o_{cat}/K_o (s^{-1} nM^{-1})
I	*L. balearicum*	9.7 ± 0.5^{ef}	346 ± 19	3.6 ± 0.1^{fg}	0.38 ± 0.01^{d}	103.3 ± 1.5^{a}	1.3	4.6
	L. barceloi	9.3 ± 0.6^{cde}	346 ± 17	3.4 ± 0.1^{f}	0.37 ± 0.03^{cd}	106.3 ± 2.0^{ab}	1.2	4.4
	L. companyonis	8.9 ± 0.3^{bcde}	429 ± 28	3.3 ± 0.2^{f}	0.37 ± 0.01^{cd}	111.8 ± 2.1^{bc}	1.4	4.2
	L. echioides	10.7 ± 0.2^{f}	427 ± 38	3.9 ± 0.1^{g}	0.37 ± 0.01^{cd}	106.4 ± 1.8^{ab}	1.5	4.4
	Average	9.7 ± 0.2^{B}	390 ± 18	3.6 ± 0.1^{B}	0.37 ± 0.01^{B}	106.7 ± 1.1^{A}	1.4 ± 0.1^{B}	4.4 ± 0.1^{B}
II	*L. ejulabilis*	7.6 ± 0.2^{ab}	415 ± 23	2.0 ± 0.2^{a}	0.26 ± 0.03^{a}	116.0 ± 3.2^{cd}	0.9	2.9
	L. grosii	8.1 ± 0.4^{abcd}	328 ± 52	2.9 ± 0.1^{de}	0.36 ± 0.01^{bcd}	113.2 ± 3.3^{bc}	1.0	4.0
	L. leonardi-llorensii	8.8 ± 0.4^{bcde}	438 ± 30	2.8 ± 0.1^{cde}	0.32 ± 0.02^{abc}	109.7 ± 1.1^{abc}	1.3	3.6
	L. magallufianum	7.0 ± 0.3^{a}	297 ± 26	2.6 ± 0.1^{cde}	0.37 ± 0.01^{cd}	110.6 ± 2.9^{bc}	1.0	4.2
	L. retusum	7.1 ± 0.4^{a}	396 ± 10	2.1 ± 0.1^{ab}	0.29 ± 0.01^{a}	121.0 ± 1.4^{d}	1.0	3.0
	Average	7.7 ± 0.2^{A}	380 ± 17	2.4 ± 0.1^{A}	0.31 ± 0.01^{A}	114.3 ± 1.3^{B}	1.0 ± 0.1^{A}	3.5 ± 0.3^{B}
III	*L. antonii-llorensii*	8.7 ± 0.3^{bcde}	397 ± 20	2.4 ± 0.1^{bc}	0.27 ± 0.01^{a}	112.1 ± 1.8^{bc}	1.1	3.1
	L. artruchium	9.4 ± 0.3^{def}	321 ± 50	3.0 ± 0.1^{e}	0.31 ± 0.02^{abc}	112.8 ± 2.0^{bc}	0.9	3.5
	L. biflorum	8.0 ± 0.3^{abc}	316 ± 19	2.4 ± 0.1^{bc}	0.30 ± 0.01^{ab}	111.9 ± 1.8^{bc}	0.8	3.4
	L. gibertii	9.1 ± 0.7^{cde}	431 ± 81	2.5 ± 0.1^{cd}	0.28 ± 0.02^{a}	112.1 ± 2.5^{bc}	1.0	3.1
	L. gymnesicum	8.2 ± 0.1^{abcd}	388 ± 15	2.4 ± 0.1^{bc}	0.29 ± 0.01^{a}	121.2 ± 2.3^{d}	0.9	3.0
	Average	8.8 ± 0.2^{AB}	368 ± 25	2.6 ± 0.1^{A}	0.29 ± 0.01^{A}	113.9 ± 1.1^{B}	0.9 ± 0.1^{A}	3.2 ± 0.1^{A}

Rubisco kinetic parameters describe the Michaelis–Menten constants for CO_2 (K_c) and O_2 (K_o), maximum rate of carboxylation (k^c_{cat}) and oxygenation (k^o_{cat}), carboxylation catalytic efficiency (k^c_{cat}/K_c), specificity factor ($S_{c/o}$), maximum rate of oxygenation (k^o_{cat}) and oxygenation catalytic efficiency (k^o_{cat}/K_o). Data are means ± SE of 3–10 replicates per species (n = 13–37 replicates per haplotype). Different lowercase and uppercase letters denote statistically significant differences by Duncan analysis ($P < 0.05$) among species and haplotypes, respectively. The maximum rate of oxygenation (k^o_{cat}) was calculated using the equation $S_{c/o} = (k^c_{cat}/K_c)/(k^o_{cat}/K_o)$.

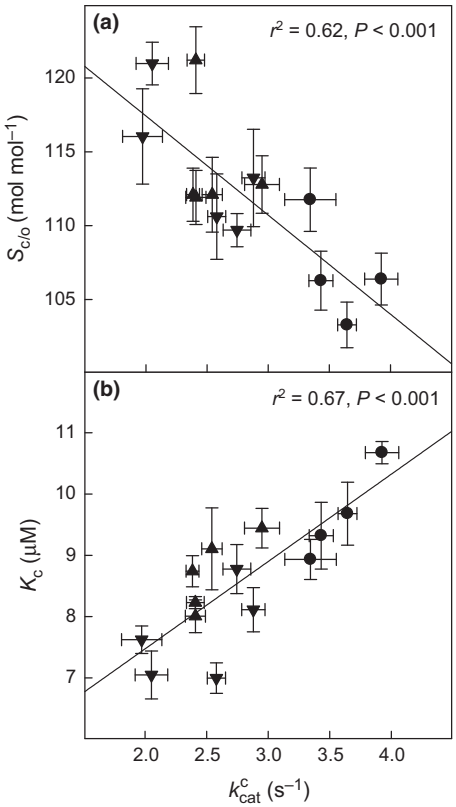

Fig. 3 Relationship between Rubisco kinetic parameters for representative species of Balearic *Limonium*. Correlation between the maximum rate of carboxylation (k^c_{cat}) and (a) the specificity factor ($S_{c/o}$) and (b) the Michaelis–Menten constant for CO_2 (K_c) is shown. All measurements were made at 25°C. Circles, haplotype I; triangles, apex down, haplotype II; triangles, apex up, haplotype III. Data are means ± SE (n = 3–10 replicates).

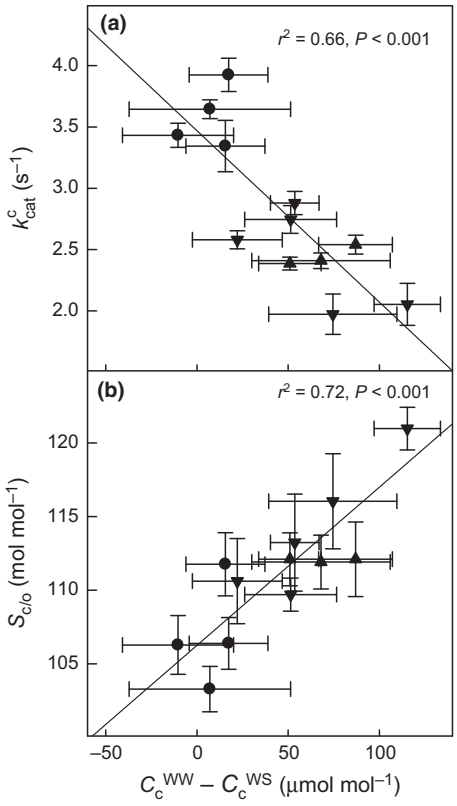

Fig. 4 Adaptation of Rubisco kinetic parameters of *Limonium* species according to the availability of CO_2 at the site of carboxylation. The relationship of the difference in the CO_2 concentration at the site of carboxylation between well-watered (C_c^{WW}) and water-stressed plants (C_c^{WS}) and (a) the maximum rate of carboxylation (k^c_{cat}) and (b) the specificity factor ($S_{c/o}$) for the 12 *Limonium* species for which *in vivo* gas exchange was measured is shown. Circles, haplotype I; triangles, apex down, haplotype II; triangles, apex up, haplotype III. Both *in vitro* and *in vivo* measurements were performed at 25°C. Data are means ± SE (n = 3–10 replicates).

the oxygenase activity always exceeded that for the carboxylase activity, leading to a decline in $S_{c/o}$. Hence, k^c_{cat} was negatively correlated with the affinity for CO_2 (i.e. $1/K_c$) and $S_{c/o}$ (Fig. 3). In other words, slower *Limonium* Rubiscos have increased specificity for CO_2. Overall, the kinetic data presented in this study are in agreement with the kinetic interrelationships described in the analysis of Savir *et al.* (2010).

The diversity in Rubisco kinetics was related to the availability of CO_2 and influenced the photosynthetic rate and biomass accumulation

The concentration of CO_2 in the chloroplast (C_c), estimated from *in vivo* measurements of leaf photosynthesis, was affected by water availability in most, but not all the species. Hence, the drought-induced decrease in C_c between WW and WS plants ($C_c^{WW} - C_c^{WS}$) was bigger in species with haplotypes II and III, and smaller in species with haplotype I Rubiscos (Fig. 4). Note that $C_c^{WW} - C_c^{WS}$ correlated negatively with k^c_{cat} ($r^2 = 0.67$; $P < 0.001$) and positively with $S_{c/o}$ ($r^2 = 0.72$; $P < 0.001$). Hence, species with haplotype I Rubisco, which showed the smallest change in C_c between WW and WS plants, had higher k^c_{cat} and lower $S_{c/o}$.

The application of severe drought stress affected both the photosynthetic capacity and biomass accumulation (B) in a species-specific manner (Fig. 5). Within each irrigation treatment, the variability in the light-saturated, gross CO_2 assimilation rate (A_G) among species correlated with differences in Rubisco kinetics. Hence, species with higher A_G had Rubisco with higher k^c_{cat} under both WW and WS (Fig. 5a). In agreement with the trade-off between k^c_{cat} and $S_{c/o}$ (Fig. 3a), A_G was inversely correlated to $S_{c/o}$ (Fig. 5b). Under WW conditions, the observed trend in the relationship between B and the same Rubisco kinetic parameters was the inverse of that with A_G, showing a negative correlation with k^c_{cat} and a positive correlation with $S_{c/o}$ (Fig. 5c,d, respectively). However, the correlation between A_G and B was not significant, either under control or under stress conditions. This apparent discrepancy serves to illustrate that isolated CO_2 exchange rates measured on individual, light-saturated leaves are not necessarily representative of the carbon flux at either whole-plant or canopy scales over the applicable growth period (120 d), particularly in plants with dense cushion-like architecture and considerable self-shading.

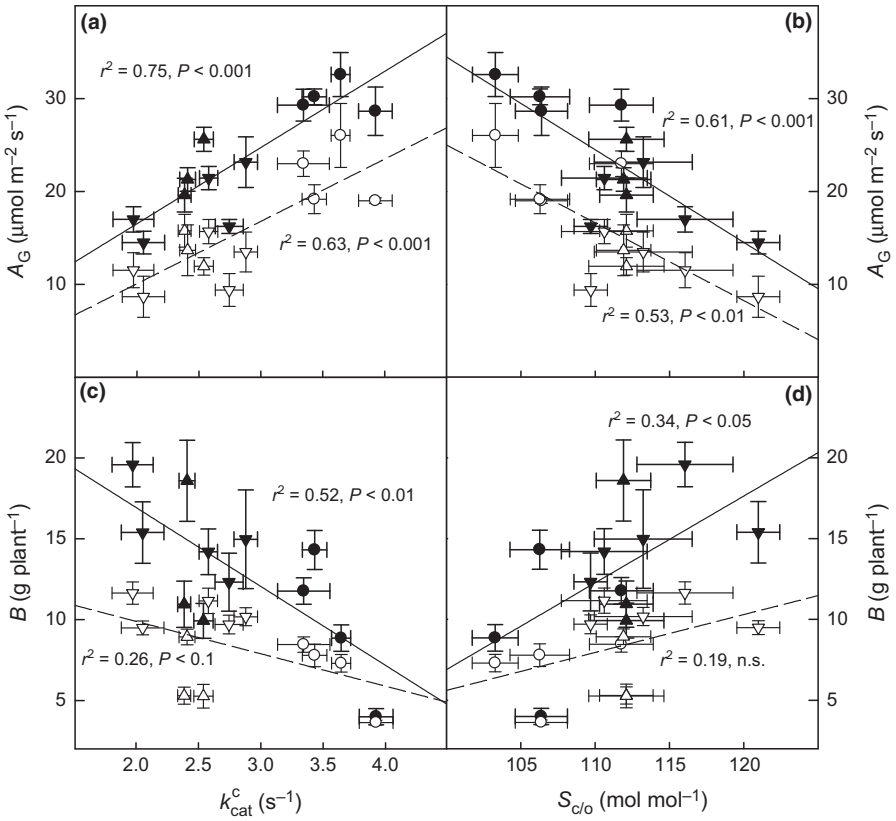

Fig. 5 Influence of Rubisco biochemistry on *in vivo* leaf photosynthesis and plant growth capacity in *Limonium*. The relationships between (a) gross CO_2 assimilation rate (A_G) and the maximum rate of carboxylation (k^c_{cat}), (b) A_G and the specificity factor ($S_{c/o}$), (c) dry biomass accumulation (B) and k^c_{cat}, and (d) B and $S_{c/o}$ are shown for the 12 *Limonium* species for which *in vivo* gas exchange was measured, under well-watered (filled symbols, solid line) and water-stress (empty symbols, dashed line) conditions. Circles, haplotype I; triangles, apex down, haplotype II; triangles, apex up, haplotype III. Both *in vitro* and *in vivo* measurements were performed at 25°C. A_G was obtained by adding half of the dark respiration rate to the net CO_2 assimilation rate. Data are means ± SE (n = 3–10 replicates). n.s., not significant.

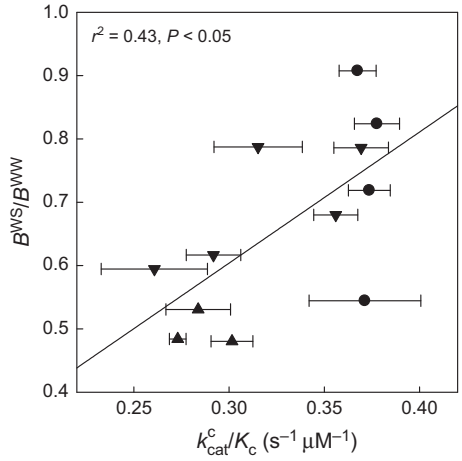

Fig. 6 Relationship between carboxylase catalytic efficiency (k^c_{cat}/K_c) and the ratio of biomass accumulation under water stress and well-watered treatments (B^{WS}/B^{WW}) for the 12 *Limonium* species for which *in vivo* gas exchange was measured. Circles, haplotype I; triangles, apex down, haplotype II; triangles, apex up, haplotype III. Data are means ± SE (n = 3–10 replicates).

The Rubisco carboxylase catalytic efficiency (k^c_{cat}/K_c) has frequently been referred to as an indicator of enzyme performance. There was a positive correlation between k^c_{cat}/K_c and the ratio of plant biomass under WS and WW conditions (Fig. 6), suggesting that the detrimental effects of drought on plant carbon gain were less in those species with higher k^c_{cat}/K_c.

Discussion

The present study shows that the stressful environments of the Mediterranean coast facilitated diversification of Rubisco within the genus *Limonium*, giving rise to three different Rubisco haplotypes coexisting in the Balearic Islands. Significantly different Rubisco kinetic properties among haplotypes were related to the differences in the concentration of CO_2 within the chloroplast stroma, and correlated not only with the photosynthetic CO_2 assimilation rate, but also with the response of plant growth to severe water stress. Rubisco L-subunit amino acid substitutions at positions 309 and 328 are likely to be responsible for the observed differences in kinetic properties, leading either to more CO_2-specific (low K_c) but slower (low k^c_{cat}) enzymes, or to less CO_2-specific (high K_c) but faster (high k^c_{cat}) forms of Rubisco. Overall, this work represents the first integrative approach linking natural polymorphisms occurring in Rubisco, its kinetic parameters, *in vivo* leaf photosynthesis and whole-plant growth, under specific environmental conditions.

Three of the observed amino acid substitutions were unique to the Balearic *Limonium* species, while the other three occurred as parallel substitutions along other branches too. The presence of the parallel amino acid substitutions is not surprising, given that all included Plumbaginaceae are drought-resistant species from Mediterranean climates with relatively similar genetic backgrounds. However, the existence of six polymorphic residues, three of which are unique to the western Mediterranean *Limonium* species, is surprisingly high

given the conservative nature of Rubisco and the short period of divergence of Balearic *Limonium* species. Complete plastome replacements via interspecific introgression have been documented for numerous plant groups (reviewed in Avise, 2004), and strong positive selection acting on chloroplast genes may facilitate this process. Interspecific hybridization is common in the Balearic *Limonium* species (Erben, 1993) resulting in cytonuclear discordance (M. À. Conesa *et al.*, unpublished data). Positive selection acting on the *rbc*L gene might have caused the three observed haplotypes to spread across all Balearic *Limonium* species. A similar situation was described for another island group, the Hawaiian *Schiedea* (Kapralov & Filatov, 2006), showing that evolution in small populations within confined geographical regions, such as islands, might be facilitated by the sharing of adaptive mutations by several closely related species.

Unlike *Flaveria* (Kubien *et al.*, 2008), which contains C_3 and C_4 species, all *Limonium* species are strictly C_3, and therefore the presence of a carbon-concentrating mechanism cannot be the factor driving Rubisco diversification, although there could be significant variation in C_c between C_3 plants (see below). Two amino acid substitutions at positions 309 and 328 were under positive selection along the branch leading to the *Limonium* species with derived haplotypes II and III, and gave rise to different Rubisco kinetics compared with the basal haplotype I. Phylogenetic analyses of the chloroplast *rbc*L gene encoding the Rubisco L-subunit showed that residues 309 and 328 were among the most frequently subjected to positive selection in both C_3 and C_4 plants (Kapralov & Filatov, 2007; Christin *et al.*, 2008; Kapralov *et al.*, 2011, 2012). Hybrid Rubisco assembling in tobacco (*Nicotiana tabacum*) plastids established that substitution M309I acted as the catalytic switch that caused the kinetic differences (similar to those reported here) between C_3 (^{309}Met) and C_4 (^{309}Ile) *Flaveria* species (Whitney *et al.*, 2011). Residue 309 is at the C-terminal end of a short β-strand (βF) at the C-terminal side of the α/β-barrel between strand 5 and helix 5 of the barrel (Fig. 2b, Table S1). This location places residue 309 on the interface of L-subunits forming a catalytic L_2 dimer. In the *Limonium* species with haplotype I (higher k_{cat}^c), residue 309 is Ile, but in haplotypes II and III (lower k_{cat}^c), it is replaced by the larger and less hydrophobic ^{309}Met (Table S1). Residue 328 is located within the loop-6 region of the α/β-barrel, which is close to the active site and has been shown to be important for catalysis and specificity (Chen & Spreitzer, 1989; Parry *et al.*, 1992). In the *Limonium* species with haplotypes II and III, polar and uncharged ^{328}Ser was replaced by the nonpolar and hydrophobic ^{328}Ala (Table S1) – a change that in other species was accompanied by an increase in $S_{c/o}$ (Chen & Spreitzer, 1989; Parry *et al.*, 1992).

The finding that haplotype I Rubiscos (^{309}Ile and ^{328}Ser) had higher k_{cat}^c (Table 1), albeit a lower affinity for CO_2 (i.e. lower $S_{c/o}$ and higher K_c) compared with the other haplotypes, is in agreement (1) with the observation of frequent positive selection at these sites (Kapralov & Filatov, 2007); and (2) with the fact that ^{309}Ile and ^{328}Ser are found in many (although not all) C_4 plants characterized by high k_{cat}^c and low affinity for CO_2 (Christin *et al.*, 2008; Kapralov *et al.*, 2011, 2012). Thus, ^{309}Ile and ^{328}Ser are likely to be among the catalytic switches for faster and less specific Rubiscos in many groups of C_3 and C_4 plants. However, their effect on the kinetic properties may vary, depending on amino acid identity at other positions, as coevolution (the attainment of similar properties by means of alternative amino acid substitutions) has been shown to be a common phenomenon in Rubisco (Wang *et al.*, 2011). Expression of recombinant *Limonium* Rubiscos in tobacco, incorporating directed mutations at these positions, may confirm their specific role in Rubisco catalysis, similar to the recent study involving *Flaveria* (Whitney *et al.*, 2011).

Although kinetic differences among haplotypes are significant, there are cases when species belonging to different haplotypes have similar kinetics despite having different Rubisco L-subunit sequences, as well as species within the same haplotype (i.e. identical L-subunit sequences) having different kinetics. One of the possible explanations for this phenomenon is differences in small subunit (S-subunit) identity and the combinations of distinct S-subunits within the Rubisco holoenzyme. Although Rubisco active sites are located in the L-subunits, S-subunits can also affect catalysis (Spreitzer, 2003). Ishikawa *et al.* (2011) showed that significant changes in Rubisco kinetics occurred when the rice (*Oryza sativa*) S-subunit was replaced with the sorghum (*Sorghum bicolor*) S-subunit. More recently, Morita *et al.* (2014) showed that Rubisco catalytic properties were influenced by the differential expression of S-subunits in rice. Hexaploid wheat, *Triticum aestivum*, possesses at least 22 *rbc*S genes encoding different S-subunits (Galili *et al.*, 1998). Many Balearic *Limonium* species are also recent polyploids (Erben, 1993), and may also possess large numbers of divergent *rbc*S genes.

The kinetic differences among haplotypes are explained on the basis of the inverse relationship between Rubisco velocity and CO_2 affinity (Fig. 3). This trade-off confirms that Rubisco evolution is flexible but essentially one-dimensional (Savir *et al.*, 2010), that is, that Rubisco may specialize towards either increased k_{cat}^c or increased $S_{c/o}$, because concomitant optimization of velocity and specificity is structurally impeded (Tcherkez, 2013). Among the potential forces driving the evolutionary adaptation of Rubisco, the availability of CO_2 for RuBP carboxylation has been crucial (Raven, 2000; Tcherkez *et al.*, 2006). This trend was confirmed in *Limonium* and other Mediterranean species inhabiting extremely xeric environments, where the low soil and atmospheric water potentials require the operation of Rubisco at low C_c for most of the growing season (Galmés *et al.*, 2013). Under these highly selective conditions, Rubisco has evolved to increase its specificity for CO_2 (Galmés *et al.*, 2005). The results in the present study clearly confirm the role exerted by C_c in shaping Rubisco kinetics. Long-term growth of *Limonium* species under severe drought stress, similar to the environmental conditions of their natural habitat, caused a significant fall in C_c in most species (Fig. 4). Under these stressful conditions, species showing the largest decrease in C_c have a more CO_2-specific Rubisco, but a lower k_{cat}^c, as a consequence of the trade-off between these properties.

On average, the fast and less CO_2-specific haplotype I Rubiscos provided higher photosynthetic capacity, although this did not translate into higher whole-plant growth (Fig. 5). This apparent discrepancy can be explained in terms of the contrasting limitations governing the CO_2 assimilation rate (A) at the leaf and whole-plant levels. Leaf-level A, which was measured at saturating light intensities during discrete gas exchange measurements, was limited by Rubisco (A_c-limited photosynthesis) in all studied species (data not shown). According to the biochemical model of leaf photosynthesis (Farquhar *et al.*, 1980), under A_c-limited photosynthesis k^c_{cat} – as part of Rubisco maximum carboxylation rate, V_{cmax} – has a decisive role in determining A. By contrast, plant biomass is the integral of temporal and spatial CO_2 assimilation and respiration processes. Given the particular plant habit of *Limonium* plants, at any given moment of the day, a large proportion of the leaves in the canopy are likely to be exposed to subsaturating sunlight. Under these conditions, whole-plant photosynthesis is predominantly limited by RuBP regeneration (A_j-limited photosynthesis), and explains why plant biomass (B) is positively correlated to $S_{c/o}$ (Fig. 5d). B did not appear to be significantly correlated to either k^c_{cat} or $S_{c/o}$ under WS (C_c decreased) but appeared to be so under WW conditions. If the ratio B^{WS}/B^{WW} is indicative of whole-plant performance under drought, it is evident (Fig. 6) that *Limonium* Rubisco with higher carboxylase catalytic efficiency (k^c_{cat}/K_c) confers greater resilience to such severe stress conditions, as demonstrated by species from haplotype I (Fig. 6).

Our study is the first to use an interdisciplinary approach to investigate the relationship between Rubisco amino acid polymorphism and catalytic efficiency, plant photosynthetic performance, growth and drought tolerance in a group of closely related C_3 species. A wide-ranging assessment of the natural diversity of Rubisco-encoding genes, together with Rubisco kinetics and its consequences for plant photosynthesis and growth under contrasting environmental conditions, will be required if knowledge-based attempts to increase global crop yields by harnessing superior forms of Rubisco are to succeed (Parry *et al.*, 2013).

Acknowledgements

This research was supported by project AGL2009-07999 (Plan Nacional, Spain) awarded to J.G. P.J.A. and M.A.J.P. are supported by the BBSRC 20:20 Wheat® Institute Strategic Program (BBSRC BB/J/00426X/1) and BBSRC BB/I002545/1 and BB/I017372/1.

References

Adler PB, Salguero-Gómez R, Compagnoni A, Hsu JS, Ray-Mukherjee J, Mbeau-Ache C, Franco M. 2014. Functional traits explain variation in plant life history strategies. *Proceedings of the National Academy of Sciences, USA* **111**: 740–745.

Agrawal AA, Fishbein M, Haliyschke R, Hastings AP, Rabosky DL, Rasmann S. 2009. Evidence for adaptive radiation from a phylogenetic study of plant defenses. *Proceedings of the National Academy of Sciences, USA* **106**: 18067–18072.

Anisimova M, Bielawski JP, Yang Z. 2001. Accuracy and power of the likelihood ratio test in detecting adaptive molecular evolution. *Molecular Biology and Evolution* **18**: 1585–1592.

Avise JC. 2004. *Molecular markers, natural history, and evolution.* Sunderland, MA, USA: Sinauer Ass.

Bracher A, Starling-Windhof A, Hartl FU, Hayer-Hartl M. 2011. Crystal structure of a chaperone-bound assembly intermediate of form I Rubisco. *Nature Structural & Molecular Biology* **18**: 875–880.

Chen Z, Spreitzer RJ. 1989. Chloroplast intragenic suppression enhances the low specificity of mutant ribulose-bisphosphate carboxylase/oxygenase. *Journal of Biological Chemistry* **264**: 3051–3053.

Christin P-A, Salamin N, Muasya AM, Roalson EH, Russier F, Besnard G. 2008. Evolutionary switch and genetic convergence on *rbcL* following the evolution of C4 photosynthesis. *Molecular Biology and Evolution* **25**: 2361–2368.

Erben M. 1993. *Limonium.* In: Castroviejo S, Aedo C, Cirujano S, Laínz M, Monserrat P, Morales R, Muñoz F, Navarro C, Paiva J, Soriano C, eds. *Flora Iberica.* Madrid, Spain: Real Jardín Botánico-CSIC, 2–143.

Esquivel MG, Genkov T, Nogueira AS, Salvucci ME, Spreitzer RJ. 2013. Substitutions at the opening of the Rubisco central solvent channel affect holoenzyme stability and CO_2/O_2 specificity but not activation by Rubisco activase. *Photosynthesis research* **118**: 209–218.

Farquhar G, von Caemmerer S, Berry J. 1980. A biochemical-model of photosynthetic CO_2 assimilation in leaves of C_3 species. *Planta* **149**: 78–90.

Flexas J, Niinemets U, Gallé A, Barbour MM, Centritto M, Díaz-Espejo A, Douthe C, Galmés J, Ribas-Carbó M, Rodríguez PL *et al.* 2013. Diffusional conductances to CO_2 as a target for increasing photosynthetic water-use efficiency. *Photosynthesis Research* **117**: 45–59.

Galili S, Avivi Y, Feldman M. 1998. Differential expression of three *RbcS* subfamilies in wheat. *Plant Science* **139**: 185–193.

Galmés J, Conesa MÀ, Ochogavía JM, Perdomo JA, Francis D, Ribas-Carbó M, Savé R, Flexas J, Medrano H, Cifre J. 2011b. Physiological and morphological adaptations in relation to water use efficiency in Mediterranean accessions of *Solanum lycopersicum*. *Plant, Cell & Environment* **34**: 245–260.

Galmés J, Flexas J, Keys AJ, Cifre J, Mitchell RAC, Madgwick PJ, Haslam RP, Medrano H, Parry MAJ. 2005. Rubisco specificity factor tends to be larger in plant species from drier habitats and in species with persistent leaves. *Plant, Cell & Environment* **28**: 571–579.

Galmés J, Kapralov MV, Andralojc PJ, Conesa MÀ, Keys AJ, Parry MAJ, Flexas J. 2014. Expanding knowledge of the Rubisco kinetics variability in plant species: environmental and evolutionary trends. *Plant, Cell & Environment.* doi: 10.1111/pce.12335.

Galmés J, Perdomo JA, Flexas J, Whitney SM. 2013. Photosynthetic characterization of Rubisco transplantomic lines reveals alterations on photochemistry and mesophyll conductance. *Photosynthesis Research* **115**: 153–166.

Galmés J, Ribas-Carbó M, Medrano H, Flexas J. 2011a. Rubisco activity in Mediterranean species is regulated by the chloroplastic CO_2 concentration under water stress. *Journal of Experimental Botany* **62**: 653–665.

Genty B, Briantais JM, Baker NR. 1989. The relationship between the quantum yield of photosynthetic electron transport and quenching of chlorophyll fluorescence. *Biochimica et Biophysica Acta* **990**: 87–92.

Harley PC, Loreto F, Di Marco G, Sharkey TD. 1992. Theoretical considerations when estimating the mesophyll conductance to CO_2 flux by analysis of the response of photosynthesis to CO_2. *Plant Physiology* **98**: 1429–1436.

Huelsenbeck JP, Ronquist F. 2001. MRBAYES: Bayesian inference of phylogenetic trees. *Bioinformatics* **17**: 754–755.

Ishikawa C, Hatanaka T, Misoo S, Miyake C, Fukayama H. 2011. Functional incorporation of sorghum small subunit increases the catalytic turnover rate of Rubisco in transgenic rice. *Plant Physiology* **156**: 1603–1611.

Kapralov MV, Filatov DA. 2006. Molecular adaptations during adaptive radiation in the Hawaiian endemic genus *Schiedea*. *PLoS ONE* **1**: e8.

Kapralov MV, Filatov DA. 2007. Widespread positive selection in the photosynthetic Rubisco enzyme. *BMC Evolutionary Biology* **7**: 73.

Kapralov MV, Kubien DS, Andersson I, Filatov DA. 2011. Changes in Rubisco kinetics during the evolution of C4 photosynthesis in *Flaveria* (Asteraceae) are associated with positive selection on genes encoding the enzyme. *Molecular Biology and Evolution* **28**: 1491–1503.

Kapralov MV, Smith JAC, Filatov DA. 2012. Rubisco evolution in C_4 eudicots: an analysis of Amaranthaceae *sensu lato*. *PLoS ONE* **7**: e52974.

Kubien DS, Whitney SM, Moore PV, Jesson LK. 2008. The biochemistry of Rubisco in *Flaveria*. *Journal of Experimental Botany* **59**: 1767–1777.

Kubitzki K, Rohwer JG, Bittrich V, Eds. 1993. *The families and genera of vascular Plants, vol. 2. Magnoliid, Hamamelid and Caryophyllid families*. Berlin Heidelberg, Germany: Springer-Verlag.

Lledó MD, Crespo MB, Fay MF, Chase MW. 2005. Molecular phylogenetics of *Limonium* and related genera (Plumbaginaceae): Biogeographical and systematic implications. *American Journal of Botany* **92**: 1189–1198.

van Lun M, Hub JS, van der Spoel D, Andersson I. 2014. CO_2 and O_2 distribution in Rubisco suggests the small subunit functions as a CO_2 reservoir. *Journal of the American Chemical Society* **136**: 3165–3171.

van Lun M, van der Spoel D, Andersson I. 2011. Subunit interface dynamics in hexadecameric rubisco. *Journal of Molecular Biology* **411**: 1083–1098.

Meyer MT, Genkov T, Skepper JN, Jouhet J, Mitchell MC, Spreitzer RJ, Griffiths H. 2012. Rubisco small-subunit α-helices control pyrenoid formation in Chlamydomonas. *Proceedings of the National Academy of Sciences, USA* **109**: 19474–19479.

Morita K, Hatanaka T, Misoo S, Fukuyama H. 2014. Unusual small subunit that is not expressed in photosynthetic cells alters the catalytic properties of Rubisco in rice. *Plant Physiology* **164**: 69–79.

Parry MAJ, Andralojc PJ, Scales JC, Salvucci ME, Carmo-Silva AE, Alonso H, Whitney SM. 2013. Rubisco activity and regulation as targets for crop improvement. *Journal of Experimental Botany* **64**: 717–730.

Parry MAJ, Madgwick PJ, Carvalho JFC, Andralojc PJ. 2007. Prospects for increasing photosynthesis by overcoming the limitations of Rubisco. *Journal of Agricultural Science* **145**: 31–43.

Parry MAJ, Madgwick P, Palmer S, Cornelius MJ, Keys AJ. 1992. Mutations in loop six of the large subunit of ribulose-1,5-bisphosphate carboxylase affect substrate specificity. *Planta* **187**: 109–112.

Parry MAJ, Reynolds M, Salvucci ME, Raines C, Andralojc PJ, Zhu XG, Price GD, Condon AG, Furbank RT. 2011. Raising yield potential of wheat. II. Increasing photosynthetic capacity and efficiency. *Journal of Experimental Botany* **62**: 453–467.

Raven JA. 2000. Land plant biochemistry. *Philosophical Transactions of the Royal Society B-Biological Sciences* **355**: 833–846.

Rosselló JA, Sáez L. 2001. Index Balearicum: an annotated check-list of the vascular plants described from the Balearic Islands. *Collectanea Botanica (Barcelona)* **25**: 1–192.

Sage RF, Kubien DS. 2007. The temperature response of C_3 and C_4 photosynthesis. *Plant, Cell & Environment* **30**: 1086–1107.

Salvucci ME, Crafts-Brandner SJ. 2004. Inhibition of photosynthesis by heat stress: the activation state of Rubisco as a limiting factor in photosynthesis. *Physiologia Plantarum* **120**: 179–186.

Savir Y, Noor E, Milo R, Tlusty T. 2010. Cross-species analysis traces adaptation of Rubisco toward optimality in a low-dimensional landscape. *Proceedings of the National Academy of Sciences, USA* **107**: 3475–3480.

Schrader SM, Wise RR, Wacholtz WF, Ort DR, Sharkey TD. 2004. Tylakoid membrane responses to moderately high leaf temeprature in Pima cotton. *Plant, Cell & Environment* **27**: 725–735.

Sharkey TD. 2005. Effects of moderate heat stress on photosynthesis: importance of thylakoid reactions, rubisco deactivation, reactive oxygen species, and thermotolerance provided by isoprene. *Plant, Cell & Environment* **28**: 269–277.

Spreitzer RJ. 2003. Role of the small subunit in ribulose-1,5-bisphosphate carboxylase/oxygenase. *Archives of Biochemistry and Biophysics* **414**: 141–149.

Spreitzer RJ, Salvucci ME. 2002. Rubisco: structure, regulatory interactions, and possibilities for a better enzyme. *Annual Review of Plant Biology* **53**: 449–475.

Tamura KD, Peterson D, Peterson N, Strecher G, Nei M, Kumar S. 2011. MEGA5: Molecular Evolutionary Genetics Analysis using maximum likelihood, evolutionary distance, and maximum parsimony methods. *Molecular Biology and Evolution* **28**: 2731–2739.

Tcherkez G. 2013. Modelling the reaction mechanisms of ribulose-1,5-bisphosphate carboxylase/oxygenase and consequences for kinetic parameters. *Plant, Cell & Environment* **36**: 1586–1596.

Tcherkez G, Farquhar GD, Andrews TJ. 2006. Despite slow catalysis and confused substrate specificity, all ribulose bisphosphate carboxylases may be nearly perfectly optimized. *Proceedings of the National Academy of Sciences, USA* **103**: 7246–7251.

Valentini R, Epron D, De Angelis P, Matteucci G, Dreyer E. 1995. *In situ* estimation of net CO_2 assimilation, photosynthetic electron flow and photorespiration in Turkey oak (*Quercus cerris* L.) leaves: diurnal cycles under different levels of water supply. *Plant, Cell & Environment* **18**: 631–640.

Wang M, Kapralov MV, Anisimova M. 2011. Coevolution of amino acid residues in the key photosynthetic enzyme Rubisco. *BMC Evolutionary Biology* **11**: 266.

Whitney SM, Sharwood RE, Orr D, White SJ, Alonso H, Galmés J. 2011. Isoleucine 309 acts as a C_4 catalytic switch that increases ribulose-1,5-bisphosphate carboxylase/oxygenase (Rubisco) carboxylation rate in *Flaveria*. *Proceedings of the National Academy of Sciences, USA* **108**: 14688–14693.

Yamori W, Noguchi K, Hikosaka K, Terashima I. 2010. Phenotypic plasticity in photosynthetic temperature acclimation among crop species with different cold tolerances. *Plant Physiology* **152**: 388–399.

Yang Z. 1997. PAML: a program package for phylogenetic analysis by maximum likelihood. *Computer Applications in the Biosciences* **13**: 555–556.

Yang Z. 2007. PAML 4: phylogenetic analysis by maximum likelihood. *Molecular Biology and Evolution* **24**: 1586–1591.

Yang Z, Wong WSW, Nielsen R. 2005. Bayes empirical Bayes inference of amino acid sites under positive selection. *Molecular Biology and Evolution* **22**: 1107–1118.

Yokota A, Canvin DT. 1985. Ribulose bisphosphate carboxylase/oxygenase content determined with [^{14}C]carboxypentitol bisphosphate in plants and algae. *Plant Physiology* **77**: 735–739.

Young JN, Rickaby REM, Kapralov MV, Filatov DA. 2012. Adaptive signals in algal Rubisco reveal a history of ancient atmospheric carbon dioxide. *Philosophical Transactions of the Royal Society B-Biological Sciences* **1588**: 483–492.

Zhang J, Kumar S. 1997. Detection of convergent and parallel evolution at the amino acid sequence level. *Molecular Biology and Evolution* **14**: 527–536.

Supporting Information

Additional supporting information may be found in the online version of this article.

Fig. S1 Phylogenetic tree inferred from the *rbc*L gene for all the *Limonium* species in the Balearic Islands.

Table S1 Changes in physical properties associated with amino acid substitutions in *Limonium rbc*L

Please note: Wiley Blackwell are not responsible for the content or functionality of any supporting information supplied by the authors. Any queries (other than missing material) should be directed to the *New Phytologist* Central Office.